Mass Spectrometry
DOI: 10.5702/massspectrometry.A0145

Technical Report

Development of a Mass Spectrometry Imaging Method to Evaluate the Penetration of Moisturizing Components Coated on Surgical Gloves into Artificial Membranes

Erika Nagano[1], Kazuki Odake[1], Toru Akiyoshi[2], and Shuichi Shimma[*,1,3,4,5]

[1]*Research and Development Department, Miruion Corporation, Ibaraki, Osaka 567–0085, Japan*
[2]*Marketing Department, Cardinal Health K.K., Tokyo 163–1035, Japan*
[3]*Department of Biotechnology, Graduate School of Engineering, Osaka University, Osaka 565–0871, Japan*
[4]*Institute for Open and Transdisciplinary Research Initiatives, Osaka University, Osaka 565–0871, Japan*
[5]*Osaka University Shimadzu Omics Innovation Research Laboratory, Osaka University, Osaka 565–0871, Japan*

Skin dryness and irritant contact dermatitis induced by the prolonged use of surgical gloves are issues faced by physicians. To address these concerns, manufacturers have introduced surgical gloves that incorporate a moisturizing component on their inner surface, resulting in documented results showing a reduction in hand dermatitis. However, the spatial distribution of moisturizers applied to surgical gloves within the integument remains unclear. Using matrix-assisted laser desorption/ionization (MALDI)–mass spectrometry imaging (MSI), we investigated the spatial distribution of moisturizers in surgical gloves within artificial membranes. Recently, dermal permeation assessments using three-dimensional models, silicone membranes, and Strat-M have gained attention as alternative approaches to animal testing. Therefore, in this study, we established an *in vitro* dermal permeation assessment of commercially available moisturizers in surgical gloves using artificial membranes. In this study, we offer a methodology to visualize the infiltration of moisturizers applied to surgical gloves into an artificial membrane using MALDI–MSI, while evaluating commercially available moisturizer-coated surgical gloves. Using our penetration evaluation method, we confirmed the infiltration of the moisturizers into the polyethersulfone 2 and polyolefin layers, which correspond to the epidermis and dermis of the skin, after the use of surgical gloves. The MSI-based method presented herein demonstrated the efficacy of evaluating the permeation of samples containing active ingredients.

Please cite this article as: Mass Spectrom (Tokyo) 2024; 13(1): A0145

Keywords: mass spectrometry imaging, artificial membranes, surgical gloves, animal substitutes, moisturizing coating compounds

(Received February 21, 2024; Accepted March 6, 2024; advance publication released online March 16, 2024)

INTRODUCTION

Surgical gloves are one of the most important personal protective equipment to protect both patients and healthcare workers from cross-infection. Skin health problems of healthcare workers due to prolonged wearing of surgical gloves are known as occupational skin disease.[1)] Irritant contact dermatitis (ICD), caused by a reduction in the skin barrier function of the hands, is a problem plaguing healthcare workers.[2–4)] Since the outbreak of the COVID-19 pandemic, approximately 80% of healthcare workers have experienced symptoms of occupational ICD.[4)] This problem not only reduces surgical performance but can also lead to healthcare-associated infections due to the colonization of normal flora on the skin of the injured hand.[5)] Therefore, ICD-related hand dermatitis is not only a skin problem but can also not be overlooked because it can increase the risk of infection and contamination. Prevention and control of hand dermatitis is closely related to the prevention of infection. Hand care with moisturizers, such as hand cream, is recommended to prevent hand dermatitis caused by ICDs.[6)] Currently, products with moisturizing ingredients coated on the inner surface of surgical gloves are available in the market. The moisturizing effect of these coated ingredients has been demonstrated by self-assessment tests by healthcare workers,

*Correspondence to: Shuichi Shimma, *Department of Biotechnology, Graduate School of Engineering, Osaka University, Osaka 565–0871, Japan*, e-mail: sshimma@bio.eng.osaka-u.ac.jp

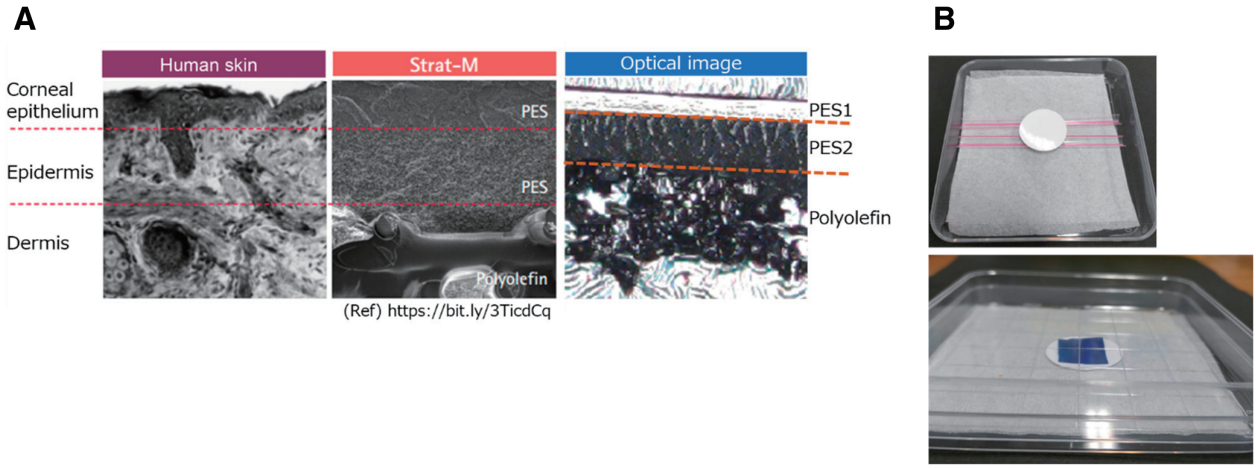

Fig. 1. (A) Comparison of the structures of the artificial membrane and human skin. Refer from https://bit.ly/3TicdCq. (B) Photographs of the permeation tests. A plastic culture dish was placed on a plastic rod and an artificial membrane was placed on top. A gap was created between the bottom of the dish and the membrane to prevent diffusion of the components that penetrated the dermis. In addition, the dish was covered with a lid to keep the surgical gloves and the artificial membrane in close contact. PES, polyethersulfone.

showing a reduction in hand dermatitis.[7] In addition, these components have been detected and quantified by liquid chromatography–mass spectrometry (LC-MS) from the stratum corneum collected by tape stripping[8,9] and from extracts of cultured skin[10]; however, these results do not indicate to which layer of the skin the moisturizing component has penetrated. Therefore, the distribution of moisturizers coated on surgical gloves in the skin remains unknown. We used matrix-assisted laser desorption/ionization (MALDI)–mass spectrometry imaging (MSI) to confirm that the moisturizer coated on surgical gloves reached the penetration of moisturizer applied to surgical gloves into the artificial membrane. We confirmed that each layer of the artificial membrane, polyethersulfone 1 (PES1), polyethersulfone 2 (PES2), and polyolefin, corresponds to the corneal epithelium, epidermis, and dermis of the skin (Fig. 1A) and that the moisturizer reached the PES2 and polyolefin layers. To date, MALDI-MSI has been used to measure skin-derived compounds, applied drugs,[11–15] and allergenic components on the surface of gloves.[16] However, there have been no measurements of the penetration of glove-coated moisturizers into the skin.

In recent years, animal testing of cosmetics has been banned in many countries and regions owing to the establishment of alternative animal testing methods. In the European Union, animal testing for cosmetics and ingredients was banned in 2013.[17,18] Similar measures are being implemented in other countries and regions, highlighting the need to develop alternative methods and ethical considerations. In addition, the Animal Welfare Law has been revised and enforced, and the 3Rs (reduction, refinement, and replacement) have been rigorously enforced. Under these circumstances, research on alternative methods for animal testing has been widely conducted, and *in vitro* skin permeation tests using three-dimensional models, silicone membranes, and Strat-M (artificial membranes) have attracted much attention.[19–35]

In this study, we used an artificial membrane in an *in vitro* skin permeation test with glycerol and panthenol, which are commonly used as moisturizing ingredients and are coating components of moisturizer-coated surgical gloves, serving as representative examples. We also investigated how moisturizing ingredients, including these two compounds, permeate the artificial membrane from a humectant-coated surgical glove.

EXPERIMENTAL

Chemicals and reagents

Lotion for use as standard and surgical gloves (Protexis PI Blue with Neu-Thera) were provided by Cardinal Health K.K. (Tokyo, Japan). 2,5-Dihydrobenzoic acid (DHB; 98% purity), α-cyano-4-hydroxycinnamic acid (CHCA), and 9-aminoacridine were purchased from Merck (Darmstadt, Germany). Platinum (Pt) was purchased from the Hitachi High-Tech Fielding Corporation (Tokyo, Japan). All solvents, including formic acid, were of LC-MS grade and purchased from Fujifilm Wako Pure Chemical Industries, Ltd. (Osaka, Japan).

Penetration test

The permeabilization procedure is illustrated in Fig. 1A. An artificial membrane (Fig. 1B; SKBM02560; Merck Millipore, MA, USA) had three thin layers. The membrane was placed on a plastic rod in a culture dish, and 200 μL lotion as a standard solution was dropped onto the PES1 side of the artificial membrane. For the surgical glove test, the inside of a 2 × 2 cm^2 surgical glove was placed in contact with the PES1 surface of the artificial membrane, and the glove was held tightly enough to prevent pressure permeation. The gloves were kept at room temperature (RT) (approximately 25°C) and 37°C (the membranes were prewarmed at 37°C), and the membranes were collected 24 and 72 h after the addition of a drop of the standard solution. Surgical gloves were collected at 18, 36, and 72 h after contact with the artificial membrane.

Sample preparation

The collected artificial membranes were quartered with an ethanol-wiped microtome blade, placed in a Cryomold No. 2 (Sakura Finetek, Tokyo, Japan) filled with 3% carboxymethyl cellulose with the PES1 layer of the artificial membrane on

top, and frozen at −80°C for 10 min to prepare the frozen block. The frozen blocks were placed on a microtome (Leica CM 1950; Leica Microsystems, GmbH, Nussloch, Germany), and 15-μm thin sections were collected on a cryofilm (2C9; SECTION-Lab, Yokohama, Japan). Sections were collected on a conductive transparent glass (indium tin oxide [ITO] glass, SI0100N without MAS coating; Matsunami Glass, Osaka, Japan) as the sample plate for MALDI-MSI, to which a conductive double-sided tape (CN4490; 3M, Tokyo, Japan) was attached. The cryofilm and surgical gloves were applied before and after the permeation treatment.

Metal coating

Surface-assisted laser desorption ionization mass spectrometry (SALDI) is increasingly used to measure nonconductive, thick samples such as surgical gloves and compounds such as glycerol that are difficult to ionize by MALDI. One problem with MALDI is that it is difficult to detect the component of interest in nonconductive, thick samples due to charge up on the intercept during ionization. It has also been found that spatial resolution and reproducibility depend on the crystals in the matrix and that reproducibility is low due to the lack of control over the crystal formation process. On the other hand, SALDI enables highly sensitive imaging of nonconductive and thick samples. Solvent-free sputtering methods using metal nanoparticles as a matrix uniformly deposit metal nanoparticles, resulting in high spatial resolution and reproducibility. Metal nanoparticles such as Ag[36,37] and Au[38] have been used as matrices in SALDI-MSI, but Pt nanoparticles have been reported to have a higher ionization efficiency than other metals.[39] It has also been reported that hybrid SALDI (matrix enhanced [ME]-Pt-SALDI) of an organic matrix and a thin metal matrix used in MALDI is highly sensitive for detecting amino acids[40] and phospholipids.[41] ME-Pt-SALDI was used for the present sample and target compounds based on this information. In order to enhance ionization efficiency of glycerol and panthenol, a Pt coating (target-to-sample distance: 30 mm, current: 25 mA, vacuum: 8 Pa, coating time: 120 s, film thickness: 20 nm) was deposited onto the ITO glass using ion sputtering (E-1045; Hitachi High-Tech Fielding Corporation).

MALDI matrix application

A CHCA matrix solution was prepared by dissolving 10 mg CHCA in 1 mL acetonitrile:ultrapure water (7:3, v/v) and adding 0.1% formic acid to the solution. Using an air brush (HT-391; WAVE), 200 μL of the CHCA matrix solution/slide was sprayed onto the Pt-coated sample plate.[42]

MALDI-MSI analysis

After a matrix layer was formed on the sample surface, measurements were performed using an iMScope TRIO (Shimadzu, Kyoto, Japan). Mass calibration was performed using DHB as the external standard. For measurements using artificial membranes, a section was cut from each of the three treated artificial membranes for each condition and the area around the center of the section (which would be the center of the treated artificial membrane) was measured. For measurements using a surgical glove, the back of the glove was cut to 2 × 2 cm and the inside measured. For the data on artificial membranes and surgical gloves, three regions were created on three artificial membranes and three regions were created on one surgical glove. Data acquisition points of 25 μm were created for each region. IMAGEREVEAL MS (Shimadzu, Kyoto, Japan) was used to extract the peak intensities from the resulting mass spectra and acquire MSI images.

Data analysis

The raw data acquired were converted to IMDX format using the IMDX Converter software. The converted IMDX files were processed using IMAGEREVEAL to extract mass spectra from the region of interest (ROI) defined at the intersection of the total ion chromatogram (TIC) image, followed by data normalization (TIC normalization) on all ROIs to obtain mass spectra independent of TIC and technical bias. Glycerol (*m/z* 115.03) or panthenol (*m/z* 228.12) was selected from this spectrum and an MS image was obtained. Statistical analysis was performed using GraphPad Prism (GraphPad Software Inc., Boston, MA, USA) and two-way analysis of variance (ANOVA) of ROI mean ion intensity values (target ion intensity of the entire ROI/number of measurement points). Standard deviations were used for error bars to show and compare data variability. We considered a difference between two samples to be significant if the significance level was less than 5% and the error bars between each sample did not overlap (small standard deviation and small scatter in the data).

RESULTS AND DISCUSSION

Imaging of standard moisturizing components in artificial membranes

Figure S1 shows the mass spectra of glycerol, panthenol, and negative control (CHCA only) using the standard samples. Figure 2 shows the distribution and peak intensities of the humectants in the artificial membrane 24 and 72 h after starting the penetration test using standard humectants. Glycerol showed no difference in distribution at RT (Fig. 2A) and 37°C (Fig. 2B), and penetration into the polyolefin was observed 24 h after the start of penetration. Panthenol showed greater penetration of the PES1 into the polyolefin at 37°C (Fig. 2D) than that at RT (Fig. 2C). The negative control results are shown in Figure S2. Panthenol remained in the PES1 24 h after the onset of penetration, whereas it penetrated the polyolefin at 72 h, indicating greater penetration into the polyolefin at 37°C than that at RT. The peak intensities in the artificial membrane under each condition are shown in Figs. 2E (glycerol) and 2F (panthenol). The mass spectra for each condition are shown in Figure S3. For both components, no significant difference in peak intensity was observed in terms of permeation time; however, there was a significant difference in peak intensity depending on the temperature. The peak intensity of penetration into the artificial membrane was significantly higher at 37°C than that at RT, suggesting that moisturizing components penetrate more easily when the temperature is closer to human body temperature. The penetration time indicated that glycerol penetrated the polyolefin more easily than panthenol. This may be because glycerol is a small compound with a molecular weight of less than 100 Da, which makes it easier to pass through the PES1 that has a barrier function. Because the PES2 and polyolefin are easily penetrated by hydrophilic compounds, glycerol and panthenol are believed to penetrate the polyolefin after passing through the PES1.

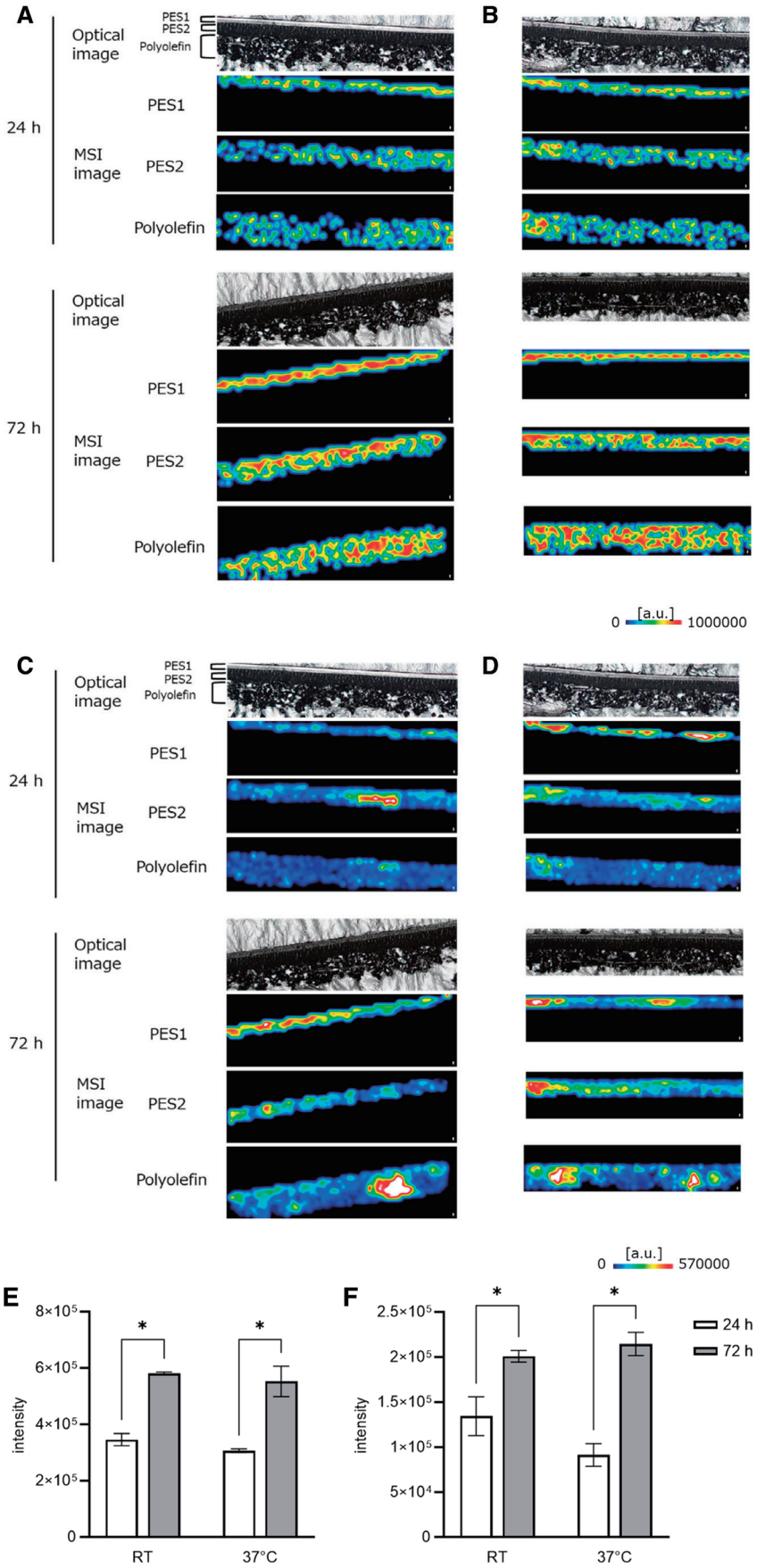

Fig. 2. Permeation of moisturizing components in artificial membranes at RT or 37°C for 24 and 72 h. (A–D) The distribution of the humectants in the membrane: glycerol at (A) RT and (B) 37°C, and panthenol at (C) RT and (D) 37°C. Glycerol has penetrated the dermis after 24 h of penetration treatment. (E and F) Comparison of the peak intensities of the (E) glycerol and (F) panthenol in the artificial membranes at RT and 37°C. The peak intensities of both compounds were significantly higher at 37°C than those at RT, but there was no difference due to the permeation time. *p <0.05, scale bar: 25 μm. a.u., astronomical unit; MSI, mass spectrometry imaging; PES, polyethersulfone; RT, room temperature.

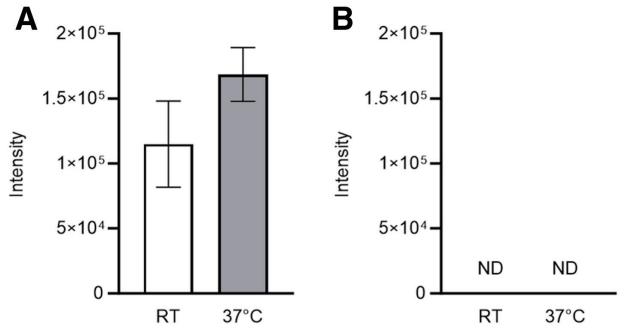

Fig. 3. Peak intensities of (A) glycerol and (B) panthenol in the artificial membranes treated at RT for 72 h with surgical gloves coated with moisturizing components. ND, not detected; RT, room temperature.

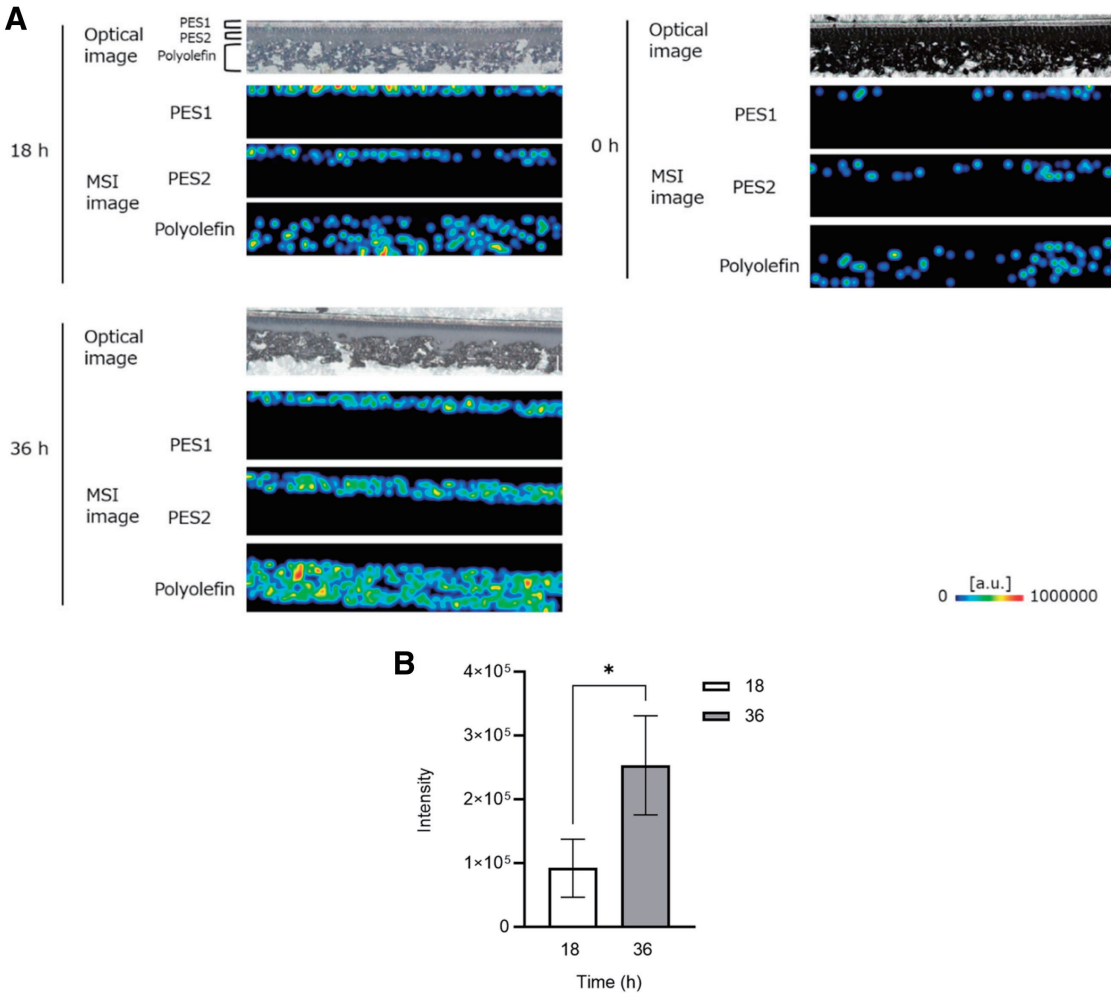

Fig. 4. Penetration of moisturizing components into artificial membranes 18 and 36 h after treatment with surgical gloves coated with moisturizing components at RT. (A) Distribution of glycerol from the surgical gloves to the membrane. After 18 h of treatment, most of the distribution was near the PES2, and at 36 h, the distribution ranged from the PES2 to the polyolefin. (B) Comparison of peak intensities. The peak intensity was significantly higher at 36 h than that at 18 h. *p <0.05, scale bar: 25 μm. a.u., astronomical unit; MSI, mass spectrometry imaging; PES, polyethersulfone; RT, room temperature.

Imaging of glove-coating moisturizing components using artificial membranes

Figure 3 shows the peak intensities of the moisturizing components in the artificial membrane 72 h after the start of the permeation test using surgical gloves coated with moisturizing components. The peak intensity of glycerol could be detected in the artificial membrane 36 h after the start of permeation, whereas that of panthenol could not be detected, even after the permeation treatment was continued for up to 72 h. The peak intensity of the moisturizing component coated on the surgical gloves in the artificial membrane did not differ significantly with temperature; however, the peak intensity tended to be higher at 37°C than that at RT. Figure 4A shows the distribution of glycerol in the artificial membrane at different penetration times. Glycerol remained in the PES1 18 h after the onset of penetration but

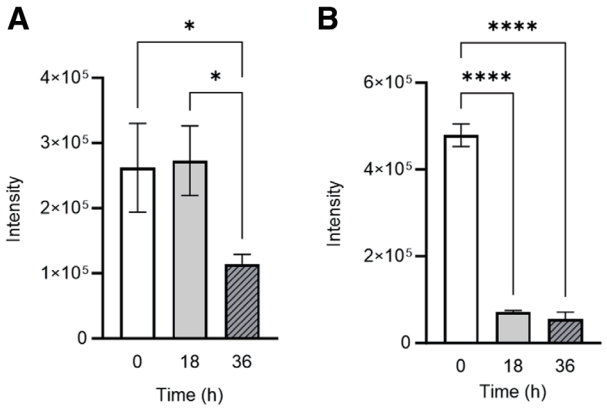

Fig. 5. Comparison of the peak intensities of the residual moisturizing components on the surface of the surgical gloves. The ion intensities of (A) glycerol and (B) panthenol were significantly decreased on the surface of surgical gloves 36 and 18 h after treatment, respectively. *p <0.05, ****p <0.0001.

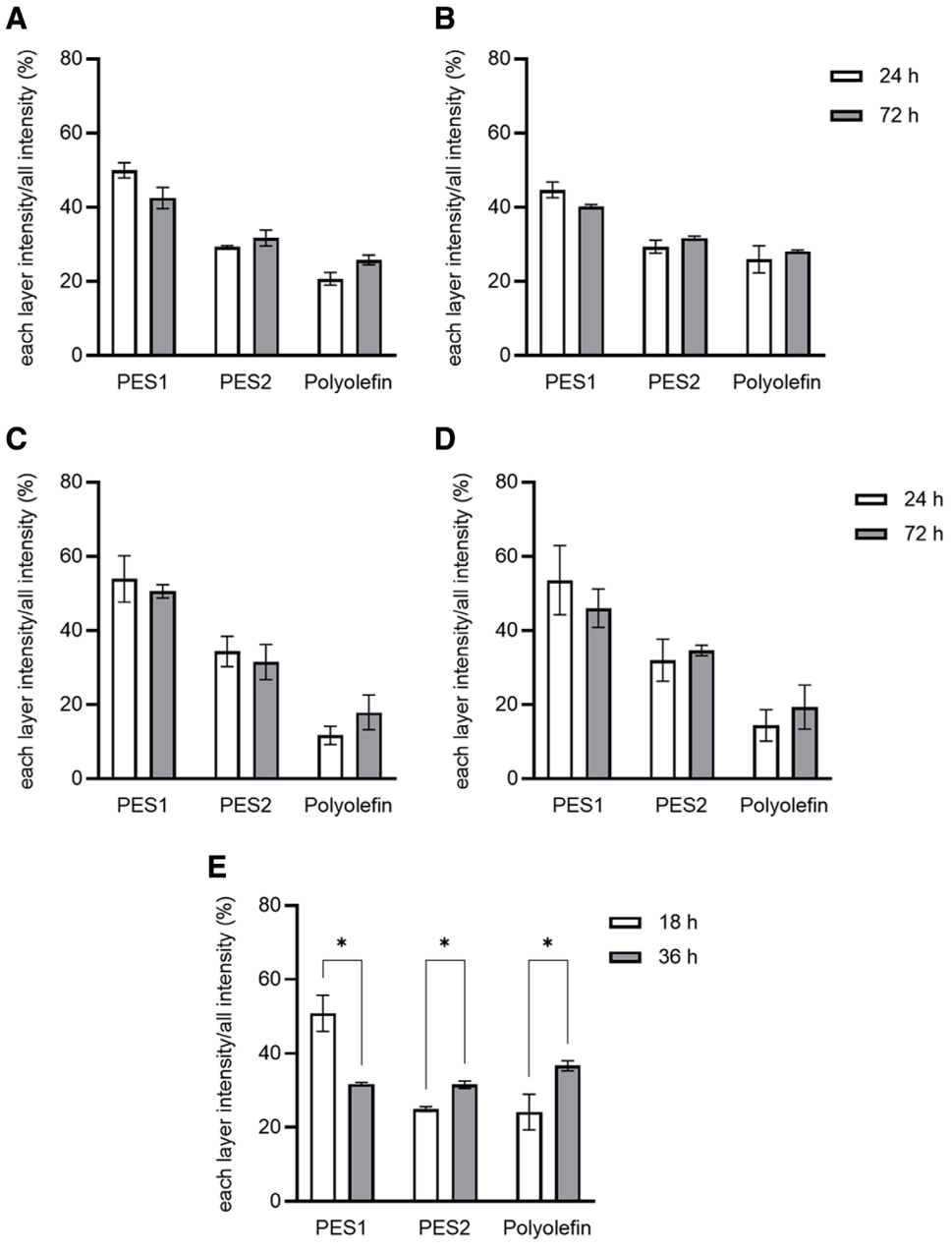

Fig. 6. Penetration evaluation results of glycerol standard at (A) RT and (B) 37°C. Penetration evaluation results of panthenol standard at (C) RT and (D) 37°C. (E) Penetration evaluation results of glycerol in a surgical glove coating. The ion intensity of each layer is expressed as a percentage of the peak intensity of the entire artificial membrane (PES1 + PES2 + polyolefin). PES, polyethersulfone; RT, room temperature.

had penetrated the polyolefin after 36 h. The peak intensity in the artificial membrane was significantly higher at 36 h than that at 18 h (Fig. 4B). To support these results, the mass spectra at each treated time are shown in Figure S4. These results suggest that the moisturizing components coated on the surgical gloves penetrate more readily at temperatures close to the human body temperature and penetrate the polyolefin over time.

Because a large percentage of the moisturizer coated on the surgical gloves was glycerol and a small percentage was panthenol, we assumed that the amount of panthenol that penetrated the artificial membrane was so small that the peak could not be detected; therefore, the remaining moisturizer component on the surgical gloves was measured. The peak intensity of glycerol on the surface of the surgical gloves decreased significantly after 36 h (Fig. 5A) and that of panthenol decreased significantly after 18 h (Fig. 5B). These results indicate that glycerol begins to permeate from the surgical gloves to the surface of the artificial membrane (PES1) at 18 h and penetrates the polyolefin at 36 h. Panthenol penetrated the membrane surface 18 h after penetration.

Evaluation of the penetration of moisturizing compounds

The ion intensity of each layer was expressed as a percentage of the peak intensity of the entire artificial membrane (PES1 + PES2 + polyolefin), and the penetration of moisturizing ingredients into each layer was evaluated (Fig. 6). Among the standard moisturizing ingredients, glycerol showed no significant difference in penetration time within the same layer; however, the percentage of glycerol in the PES2 and polyolefin tended to increase from 36 to 72 h, whereas the percentage in the PES1 decreased (Figs. 6A and 6B). Panthenol also showed no significant difference in penetration time in the same layer, but the percentage of panthenol in the polyolefin tended to increase at 72 h compared with that at 36 h (Fig. 6C). The percentage of panthenol in the PES2 was higher at 37°C (Fig. 6D) than that at RT (Fig. 6C). Under both temperature conditions, the percentage of panthenol in the PES1 decreased over time. These results indicate that the standard moisturizing ingredients penetrate the PES1 and reach the polyolefin over time. The percentage of glycerol penetrating the membrane from the surgical gloves is shown in Fig. 6E. The percentage of glycerol in the PES1 at 36 h was lower than that at 18 h, whereas the percentages in the PES2 and polyolefin increased significantly. These results indicate that glycerol penetrated inward from the PES1 and reached the PES2 with contact time.

In this study, we proposed a method to visualize and evaluate the distribution of glycerol, a moisturizing component coated on surgical gloves, in artificial membranes using MSI. After contact between the surgical gloves and artificial membrane, glycerol penetrates the PES1 and is distributed in the PES2 and polyolefin. The peak intensity decreased over time on the surface of the surgical gloves and increased over time on the membrane. These results suggest that glycerol penetrated the artificial membrane. The method presented in this study is expected to be viable for evaluating the permeation of samples containing active ingredients, such as the distribution of active ingredients in patch drugs.

ACKNOWLEDGMENT

In this study, we used Co-Labo Maker, a research resource-sharing platform. Co-Labo Maker Inc. provided intermediary support for the establishment of this research topic, research design, and construction of the process through an implementation evaluation. We would like to thank the Co-Labo Maker team.

SUPPORTING INFORMATION

Supporting information is available at the online article sites on J-STAGE and PMC.

REFERENCES

1) S. Skotnicki. *The Workplace Safety and Insurance Appeals Tribunal,* 2008 (https://www.wsiat.on.ca/en/MedicalDiscussionPapers/allergic.pdf).
2) E. Proksch, J. M. Brandner, J. M. Jensen. The skin: An indispensable barrier. *Exp. Dermatol.* 17: 1063–1072, 2008.
3) A. V. Rawlings. Recent advances in skin 'barrier' research. *J. Pharm. Pharmacol.* 62: 671–677, 2010.
4) L. F. Kiely, E. Moloney, G. O'Sullivan, J. A. Eustace, J. Gallagher, J. F. Bourke. Irritant contact dermatitis in healthcare workers as a result of the COVID-19 pandemic: A cross-sectional study. *Clin. Exp. Dermatol.* 46: 142–144, 2021.
5) E. L. Larson, C. A. Norton Hughes, J. D. Pyrek, S. M. Sparks, E. U. Cagatay, J. M. Bartkus. Changes in bacterial flora associated with skin damage on hands of health care personnel. *Am. J. Infect. Control* 26: 513–521, 1998.
6) J. M. Boyce, D. Pittet; Healthcare Infection Control Practices Advisory Committee; HICPAC/SHEA/APIC/IDSA Hand Hygiene Task Force; Society for Healthcare Epidemiology of America/Association for Professionals in Infection Control/Infectious Diseases Society of America. Guideline for hand hygiene in health-care settings. Recommendations of the Healthcare Infection Control Practices Advisory Committee and the HICPAC/SHEA/APIC/IDSA Hand Hygiene Task Force. Society for Healthcare Epidemiology of America/Association for Professionals in Infection Control/Infectious Diseases Society of America. *MMWR Recomm. Rep.* 51(RR-16): 1–45, quiz, CE1-CE4, 2002.
7) D. D. Davis, R. A. Harper. Using gloves coated with a dermal therapy formula to improve skin condition. *AORN J.* 81: 157–166, 2005.
8) G. Hochart, D. Bonnel, J. Stauber, G. N. Stamatas. Biomarker mapping on skin tape strips using MALDI mass spectrometry imaging. *J. Am. Soc. Mass Spectrom.* 30: 2082–2091, 2019.
9) T. Kezutyte, N. Desbenoit, A. Brunelle, V. Briedis. Studying the penetration of fatty acids into human skin by ex vivo TOF-SIMS imaging. *Biointerphases* 8: 3, 2013.
10) B. De Spiegeleer, J. Boonen, S. V. Malysheva, J. D. Mavungu, S. De Saeger, N. Roche, P. Blondeel, L. Taevernier, L. Veryser. Skin penetration enhancing properties of the plant N-alkylamide spilanthol. *J. Ethnopharmacol.* 148: 117–125, 2013.
11) V. Čižinauskas, N. Elie, A. Brunelle, V. Briedis. Fatty acids penetration into human skin ex vivo: A TOF-SIMS analysis approach. *Biointerphases* 12: 011003, 2017.
12) P. Sjövall, T. M. Greve, S. K. Clausen, K. Moller, S. Eirefelt, B. Johansson, K. T. Nielsen. Imaging of distribution of topically applied drug molecules in mouse skin by combination of time-of-flight secondary ion mass spectrometry and scanning electron microscopy. *Anal. Chem.* 86: 3443–3452, 2014.
13) C. Russo, N. Brickelbank, C. Duckett, S. Mellor, S. Rumbelow, M. R. Clench. Quantitative investigation of terbinafine hydrochloride absorption into a living skin equivalent model by MALDI-MSI. *Anal. Chem.* 90: 10031–10038, 2018.
14) I. S. Sørensen, C. Janfelt, M. M. B. Nielsen, R. W. Mortensen, N. Ø. Knudsen, A. H. Eriksson, A. J. Pedersen, K. T. Nielsen.

Combination of MALDI-MSI and cassette dosing for evaluation of drug distribution in human skin explant. *Anal. Bioanal. Chem.* 409: 4993–5005, 2017.
15) D. Bonnel, R. Legouffe, A. H. Eriksson, R. W. Mortensen, F. Pamelard, J. Stauber, K. T. Nielsen. MALDI imaging facilitates new topical drug development process by determining quantitative skin distribution profiles. *Anal. Bioanal. Chem.* 410: 2815–2828, 2018.
16) M. Marchetti-Deschmann, G. Allmaier. Allergenic compounds on the inner and outer surfaces of natural latex gloves: MALDI mass spectrometry and imaging of proteinous allergens. *J. Mass Spectrom.* 44: 61–70, 2009.
17) M. Lodén, L. Ungerth, J. Serup. Changes in European legislation make it timely to introduce a transparent market surveillance system for cosmetics. *Acta Derm. Venereol.* 87: 485–492, 2007.
18) H. Spielmann. Animal use in the safety evaluation of chemicals: Harmonization and emerging needs. *ILAR J.* 43(Suppl_1): S11–S17, 2002.
19) C. E. Spencer, L. E. Flint, C. J. Duckett, L. M. Cole, N. Cross, D. P. Smith, M. R. Clench. Role of MALDI-MSI in combination with 3D tissue models for early stage efficacy and safety testing of drugs and toxicants. *Expert Rev. Proteomics* 17: 827–841, 2020.
20) A. Harvey, L. M. Cole, R. Day, M. Bartlett, J. Warwick, R. Bojar, D. Smith, N. Cross, M. R. Clench. MALDI-MSI for the analysis of a 3D tissue-engineered psoriatic skin model. *Proteomics* 16: 1718–1725, 2016.
21) M. Feucherolles, W. Le, J. Bour, C. Jacques, H. Duplan, G. Frache. A comprehensive comparison of tissue processing methods for high-quality MALDI imaging of lipids in reconstructed human epidermis. *J. Am. Soc. Mass Spectrom.* 34: 2469–2480, 2023.
22) D. C. Hammell, E. I. Stolarczyk, M. Klausner, M. O. Hamad, P. A. Crooks, A. L. Stinchcomb. Bioconversion of naltrexone and its 3-O-alkyl-ester prodrugs in a human skin equivalent. *J. Pharm. Sci.* 94: 828–836, 2005.
23) S. Gabbanini, E. Lucchi, M. Carli, E. Berlini, A. Minghetti, L. Valgimigli. In vitro evaluation of the permeation through reconstructed human epidermis of essentials oils from cosmetic formulations. *J. Pharm. Biomed. Anal.* 50: 370–376, 2009.
24) S. Madiedo-Podvrsan, J. P. Belaïdi, S. Desbouis, L. Simonetti, Y. Ben-Khalifa, C. Collin-Djangone, J. Soeur, M. Rielland. Utilization of patterned bioprinting for heterogeneous and physiologically representative reconstructed epidermal skin models. *Sci. Rep.* 11: 6217, 2021.
25) G. Ottaviani, S. Martel, P. A. Carrupt. In silico and in vitro filters for the fast estimation of skin permeation and distribution of new chemical entities. *J. Med. Chem.* 50: 742–748, 2007.
26) G. Lian, L. Chen, L. Han. An evaluation of mathematical models for predicting skin permeability. *J. Pharm. Sci.* 97: 584–598, 2008.
27) R. Zeng, J. Deng, L. Dang, X. Yu. Correlation between the structure and skin permeability of compounds. *Sci. Rep.* 11: 10076, 2021.
28) S. Geinoz, R. H. Guy, B. Testa, P. A. Carrupt. Quantitative structure-permeation relationships (QSPeRs) to predict skin permeation: A critical evaluation. *Pharm. Res.* 21: 83–92, 2004.
29) T. Hatanaka, M. Inuma, K. Sugibayashi, Y. Morimoto. Prediction of skin permeability of drugs. I. Comparison with artificial membrane. *Chem. Pharm. Bull.* 38: 3452–3459, 1990.
30) R. Roguet, C. Cohen, C. Robles, P. Courtellemont, M. Tolle, J. P. Guillot, X. Pouradier Duteil. An interlaboratory study of the reproducibility and relevance of Episkin, a reconstructed human epidermis, in the assessment of cosmetics irritancy. *Toxicol. In Vitro* 12: 295–304, 1998.
31) E. Abd, S. A. Yousef, M. N. Pastore, K. Telaprolu, Y. H. Mohammed, S. Namjoshi, J. E. Grice, M. S. Roberts. Skin models for the testing of transdermal drugs. *Clin. Pharmacol.* 8: 163–176, 2016.
32) A. A. Reus, K. Reisinger, T. R. Downs, G. J. Carr, A. Zeller, R. Corvi, C. A. Krul, S. Pfuhler. Comet assay in reconstructed 3D human epidermal skin models--Investigation of intra- and inter-laboratory reproducibility with coded chemicals. *Mutagenesis* 28: 709–720, 2013.
33) I. C. Roseboom, B. Thijssen, H. Rosing, F. Alves, D. Mondal, M. B. M. Teunissen, J. H. Beijnen, T. P. C. Dorlo. Development and validation of an HPLC-MS/MS method for the quantification of the anti-leishmanial drug miltefosine in human skin tissue. *J. Pharm. Biomed. Anal.* 207: 114402, 2022.
34) I. C. Roseboom, H. Rosing, J. H. Beijnen, T. P. C. Dorlo. Skin tissue sample collection, sample homogenization, and analyte extraction strategies for liquid chromatographic mass spectrometry quantification of pharmaceutical compounds. *J. Pharm. Biomed. Anal.* 191: 113590, 2020.
35) E. Sutterby, P. Thurgood, S. Baratchi, K. Khoshmanesh, E. Pirogova. Evaluation of in vitro human skin models for studying effects of external stressors and stimuli and developing treatment modalities. *VIEW* 3: 20210012, 2022.
36) G. McCombie, R. Knochenmuss. Enhanced MALDI ionization efficiency at the metal-matrix interface: Practical and mechanistic consequences of sample thickness and preparation method. *J. Am. Soc. Mass Spectrom.* 17: 737–745, 2006.
37) S. Cha, Z. Song, B. J. Nikolau, E. S. Yeung. Direct profiling and imaging of epicuticular waxes on *Arabidopsis thaliana* by laser desorption/ionization mass spectrometry using silver colloid as a matrix. *Anal. Chem.* 81: 2991–3000, 2009.
38) T. Hayasaka, N. Goto-Inoue, N. Zaima, K. Shrivas, Y. Kashiwagi, M. Yamamoto, M. Nakamoto, M. Setou. Imaging mass spectrometry with silver nanoparticles reveals the distribution of fatty acids in mouse retinal sections. *J. Am. Soc. Mass Spectrom.* 21: 1446–1454, 2010.
39) N. Goto-Inoue, T. Hayasaka, N. Zaima, Y. Kashiwagi, M. Yamamoto, M. Nakamoto, M. Setou. The detection of glycosphingolipids in brain tissue sections by imaging mass spectrometry using gold nanoparticles. *J. Am. Soc. Mass Spectrom.* 21: 1940–1943, 2010.
40) T. Yonezawa, H. Kawasaki, A. Tarui, T. Watanabe, R. Arakawa, T. Shimada, F. Mafuné. Detailed investigation on the possibility of nanoparticles of various metal elements for surface-assisted laser desorption/ionization mass spectrometry. *Anal. Sci.* 25: 339–346, 2009.
41) J.-Y. Noh, M.-J. Kim, J.-M. Park, T.-G. Yun, M.-J. Kang, J.-C. Pyun. Laser desorption/ionization mass spectrometry of L-thyroxine (T_4) using combi-matrix of α-cyano-4-hydroxycinnamic acid (CHCA) and graphene. *J. Anal. Sci. Technol.* 13: 5, 2022.
42) T. Ozawa, I. Osaka, T. Ihozaki, S. Hamada, Y. Kuroda, T. Murakami, A. Miyazato, H. Kawasaki, R. Arakawa. Simultaneous detection of phosphatidylcholines and glycerolipids using matrix-enhanced surface-assisted laser desorption/ionization-mass spectrometry with sputter-deposited platinum film. *J. Mass Spectrom.* 50: 1264–1269, 2015.